IL NUOVO CIMENTO Vol. 36 C, N. 6 Novembre-Dicembre 2013
DOI 10.1393/ncc/i2014-11627-4

Colloquia: LaThuile13

B_c physics at LHCb

L. Anderlini on behalf of the LHCb Collaboration
INFN, Sezione di Firenze - Sesto Fiorentino (FI), Italy and
European Organization for Nuclear Research (CERN) - Meyrin, Geneva, Switzerland

ricevuto il 20 Giugno 2013; approvato l'1 Luglio 2013

Summary. — The B_c^+ meson is unique in the standard model as it is the ground state of a family of mesons containing two different heavy flavour quarks. Recent results on the B_c^+ state are discussed and prospects of B_c studies at LHCb are described. Using the large data sample collected in 2011 at $\sqrt{s} = 7\,\text{TeV}$, the LHCb Collaboration achieved precise mass and production measurement of the B_c^+ meson and reported the first observation of the $B_c^+ \to J/\psi\,\pi^+\pi^-\pi^+$ and $B_c^+ \to \psi(2S)\,\pi^+$ decay modes. Their branching fractions relative to $B_c^+ \to J/\psi\pi^+$ are measured. Future studies on B_c excited states will provide a relevant input to the theoretical models of QCD-bound states involving two heavy quarks.

PACS 14.40.Pq – Heavy quarkonia.
PACS 14.40.Nd – Bottom mesons.
PACS 14.40.Lb – Charmed mesons.

1. – Introduction

The B_c^+ meson is the ground state of the $\bar{b}c$ quark pair system([1]). It is the only known meson composed of two different heavy flavoured quarks (charm and bottom quark).

Studies on B_c mesons can be divided in three main domains: production, spectroscopy and decay modes; in the following, they are briefly introduced before illustrating the LHCb results.

1˙1. *Production.* – At $\sqrt{s} = 7\,\text{TeV}$, the most probable way to produce $B_c^{(*)+}$ mesons is through gg-fusion process, $gg \to B_c^{(*)+} + b + \bar{c}$ [1]. According to a complete α_s^4 calculation, the production cross-section of the B_c^+ is predicted to be about $0.4\,\mu\text{b}$ in pp collisions at $\sqrt{s} = 7\,\text{TeV}$ including contribution from excited states [2]. At the Tevatron energy $\sqrt{s} = 1.96\,\text{TeV}$, in $p\bar{p}$ collisions, the B_c^+ production cross-section is expected to be one order of magnitude lower. The production of B_c mesons is forbidden at the b-factories, in e^+e^- collisions.

([1]) Charge conjugate states are implied through this contribution.

The theoretical predictions suffer from large uncertainties, and an accurate measurement of the B_c^+ production cross-section is needed to guide the experimental studies at the LHC.

1˙2. *Spectroscopy.* – Potential models predict the spectrum of the B_c mesons to be similar to that of quarkonium states (see for example [3]). The only state experimentally observed is the ground state B_c^+ for which potential models predict a mass between 6.2 and $6.4\,\mathrm{GeV}/c^2$ [1], perturbative QCD methods lead to a prediction of $6326^{+29}_{-9}\,\mathrm{MeV}/c^2$ [4]. Finally, lattice QCD predicts the B_c^+ mass to be $6278 \pm 6 \pm 4\,\mathrm{MeV}/c^2$, in excellent agreement with the world average: $6277 \pm 6\,\mathrm{MeV}/c^2$ [5].

1˙3. *Decay modes.* – While the decay of B_c excited states is dominated by electromagnetic and strong modes, the ground state can only decay weakly. Up to now, only decays due to the $\bar{b} \to \bar{c}$ transition have been observed. The $c\bar{c}$ pair in the final state often originates a J/ψ which can be easily detected and reconstructed when decaying to two leptons. The experimental benefit from J/ψ in the final state is so important that decay channels due to the $c \to s$ transition, although Cabbibo favored with respect to $\bar{b} \to \bar{c}$, have never been observed. They are likely to have a B_s^0 in the final state which is harder to reconstruct than dileptons. Finally, the B_c^+ meson can decay through weak annihilation $\bar{b}c \to W^*$, CKM-favored with respect to $\bar{b}u \to W^*$ transitions in B^+ decays.

The lifetime of the B_c^+ state is expected to be 0.48 ± 0.05 ps using the QCD sum-rules formalism, while the world average is 0.45 ± 0.04 ps [5].

2. – LHCb detector

The LHCb detector, described elsewhere in these proceedings [6] and in more detail in [7], is a single-arm forward spectrometer covering the pseudorapidity range $2 < \eta < 5$. It ran at instantaneous luminosity of $3.5 \times 10^{32}\,\mathrm{cm}^{-1}\mathrm{s}^{-1}$ in 2011 and $4.5 \times 10^{32}\,\mathrm{cm}^{-1}\mathrm{s}^{-1}$ in 2012.

Event online selection relies on a trigger system consisting of a hardware stage, based on information from the calorimeter and muon systems, followed by a software stage which applies a full event reconstruction. The hardware trigger plays an important role in selecting events with a J/ψ in the final state, selecting events with a single muon candidate or a pair of muon candidates having high transverse momenta. At the successive software trigger stage, candidates are required to have a pair of tracks identified as muons with invariant mass within $120\,\mathrm{MeV}/c^2$ of the J/ψ mass [5].

Signal efficiencies, including geometrical acceptance, reconstruction, selection and trigger effects are determined using simulated signal events. While the *pp* collision is described with PYTHIA 6.4 [12], as well as the production of B^+ mesons, the production of B_c states is described using the dedicated Monte Carlo generator BCVECPY [11]. Decays of B_c^+, B^+ and J/ψ mesons are described with EVTGEN [13] in which the final state radiation is generated using PHOTOS [14].

3. – B_c^+ mass and production cross-section measurement

The measurement of mass and production cross-section of the B_c^+ meson is reported on [8], and relies on a $370\,\mathrm{pb}^{-1}$ of integrated luminosity collected in 2011 at $\sqrt{s} = 7\,\mathrm{TeV}$ by the LHCb experiment. The $B_c^+ \to J/\psi\pi^+$ (signal) and $B^+ \to J/\psi K^+$ (control) decay modes are topological identical and are selected with requirements as similar as possible to each other.

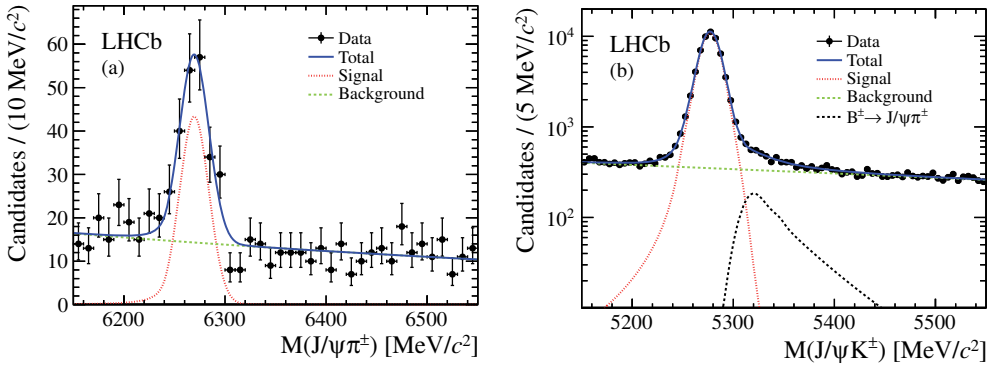

Fig. 1. – Invariant mass distribution of selected (a) $B_c^+ \to J/\psi\pi^+$ candidates and (b) $B^+ \to J/\psi K^+$ candidates, used in the production measurements. The fits to the data are superimposed.

After the online selection, in order to improve the B_c^+ and B^+ mass resolutions, the mass of the $\mu^+\mu^-$ pair is constrained to the J/ψ mass, and the b-meson candidates are required to have decay time $t > 0.25\,\text{ps}$ to reject the important background due to the combination of a prompt J/ψ and a prompt pion from the same primary vertex.

3˙1. *The production cross-section measurement.* – A further selection is applied when measuring the cross section, defining a fiducial region requiring the b-meson to have $p_T > 4\,\text{GeV}$ and pseudorapidity in the range $2.5 < \eta < 4.5$. The fiducial region is chosen to be well inside the detector acceptance to have a reasonably flat efficiency over the phase-space.

The yields for the signal and the control samples are obtained from extended unbinned maximum-likelihood fits to the invariant mass distributions of the reconstructed B_c^+ and B^+ candidates. The $B_c^+ \to J/\psi\pi^+$ signal shape is described by a double-sided Crystal Ball function [9]. The $B^+ \to J/\psi K^+$ signal mass shape is described by the sum of two double-sided Crystal Ball functions wih the same mass and different resolutions. The combinatorial background is described by an exponential function. Background to $B^+ \to J/\psi K^+$ due to Cabibbo-suppressed $B^+ \to J/\psi\pi^+$ decays is included to improve the fit quality. The distribution is determined from the simulated events, while the ratio of the number of $B_c^+ \to J/\psi\pi^+$ decays to that of the signal is fixed to $\mathcal{B}(B^+ \to J/\psi\pi^+)/\mathcal{B}(B^+ \to J/\psi K^+) = 3.83\%$ [10]. The Cabibbo-suppressed decay $B_c^+ \to J/\psi K^+$ is neglected as a source of background for $B_c^+ \to J/\psi\pi^+$. Figure 1 shows the invariant mass distributions of the selected $B_c^+ \to J/\psi\pi^+$, the fitted models are superimposed.

The numbers of signal events are 162 ± 18 for $B_c^+ \to J/\psi\pi^+$ and 56243 ± 256 for $B^+ \to J/\psi K^+$ as obtained from the fit.

The ratio of the production cross-section times branching fraction measured in this analysis is then

$$R_{c/u} = \frac{\sigma(B_c^+)\mathcal{B}(B_c^+ \to J/\psi\pi^+)}{\sigma(B^+)\mathcal{B}(B^+ \to J/\psi K^+)} = \frac{N(B_c^+ \to J/\psi\pi^+)}{\varepsilon_{tot}^c} \frac{\varepsilon_{tot}^u}{N(B^+ \to J/\psi K^+)},$$

where $\sigma(B_c^+)$ and $\sigma(B^+)$ are the inclusive production cross-sections of B_c^+ and B^+ mesons

in pp collisions at $\sqrt{s} = 7\,\text{TeV}$, $\mathcal{B}(B_c^+ \to J/\psi\pi^+)$ and $\mathcal{B}(B^+ \to J/\psi K^+)$ are the branching fractions of the reconstructed decay chains, $N(B_c^+ \to J/\psi\pi^+)$ and $N(B^+ \to J/\psi K^+)$ are the yields of the $B_c^+ \to J/\psi\pi^+$ and $B^+ \to J/\psi K^+$ signal decays, and ε_{tot}^c and ε_{tot}^u are the total efficiencies, including geometrical acceptance, reconstruction, selection, and trigger effects, for B_c^+ and B^+ respectively.

The procedure described above leads to $R_{c/u} = (0.68 \pm 0.10)\%$, where the uncertainty is statistical only. The evaluation of systematics is detailed elsewhere [8], the dominant contributions is the uncertainty on the B_c^+ lifetime, which has been measured by CDF [15] and D0 [16] to give $\tau(B_c^+) = 0.453 \pm 0.041\,\text{ps}$ [5]. The uncertainty on the lifetime results in an uncertainty on the efficiency of the detachment cut, and therefore on the measurement of the number of produced B_c^+.

The effects of the trigger requirements have been evaluated by only using events triggered by the lifetime unbiased (di)muon lines. Repeating the complete analysis, a ratio of $R_{c/u} = (0.65 \pm 0.10)\%$ is found, resulting in a systematic uncertainty of 4%.

Other considered systematic uncertainties are due to the chosen fit model for signal and combinatorial background, the tracking efficiency difference between data and simulation, the effect of hadron interaction on the reconstructed tracks, and the choice of the (p_T, η) binning. Combining all the systematic uncertainties in quadrature, we obtain $R_{c/u} = (0.68 \pm 0.10\ (\text{stat}) \pm 0.03\ (\text{syst}) \pm 0.05\ (\text{lifetime}))\%$ for B_c^+ and B^+ mesons with transverse momenta $p_T > 4\,\text{GeV}/c$ and pseudorapidities $2.5 < \eta < 4.5$. Ongoing analyses at LHCb aim to a new and more precise measurement of the B_c^+ lifetime.

3˙2. *The mass measurement.* – The mass measurement relies on a slightly different selection optimised to reduce mass bias and enhance efficiency and signal-to-noise ratio. All events are used regardless of the trigger line and the fiducial region is removed. Only candidates with a good measured mass uncertainty are used, and a loose particle identification requirement is introduced to remove the small contamination from $B_c^+ \to J/\psi K^+$ decays.

The B_c^+ mass is determined with an extended maximum-likelihood fit to the invariant mass distribution of the selected $B_c^+ \to J/\psi\pi^+$ candidates. The mass difference $M(B_c^+) - M(B^+)$ is obtained by fitting the invariant mass distribution of the selected $B_c^+ \to J/\psi\pi^+$ and $B^+ \to J/\psi K^+$ decays.

The B_c^+ mass is determined to be $6273.0 \pm 1.3\,\text{MeV}/c^2$ with a resolution of $13.4 \pm 1.1\,\text{MeV}/c^2$, and the mass difference $M(B_c^+) - M(B^+)$ is $994.3 \pm 1.3\,\text{MeV}/c^2$. The uncertainties are statistical only.

Systematic uncertainties due to the invariant mass model, momentum scale calibration, detector description and alignment are assessed by repeating the complete analysis including the momentum scale calibration and track fit by changing parameters to which the mass distribution is sensitive within their uncertainty. Deviations from the nominal value of the B_c^+ mass are reported as systematic uncertainties. The total systematic uncertainty, obtained as quadratic sum of the various contributions, is $1.6\,\text{MeV}/c^2$ on the B_c^+ mass and $0.6\,\text{MeV}/c^2$ on the B_c^+-B^+ mass difference.

4. – First observation of the decay $B_c^+ \to J/\psi\pi^+\pi^-\pi^+$

The decay $B_c^+ \to J/\psi\pi^+\pi^-\pi^+$ has been observed [17] for the first time using $0.8\,\text{fb}^{-1}$ of pp collision at $\sqrt{s} = 7\,\text{TeV}$ collected by the LHCb expertiment in 2011. The branching fraction for this decay is expected to be 1.5–2.3 times higher than for $B_c^+ \to J/\psi\pi^+$ [19].

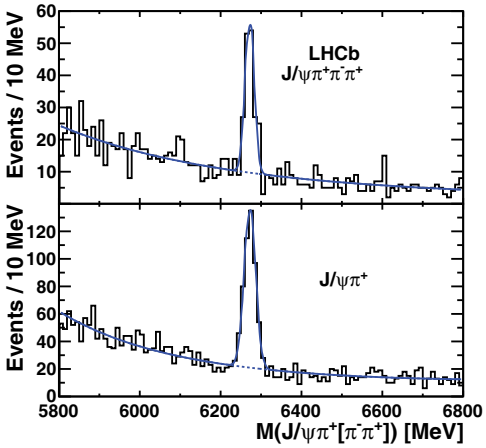

Fig. 2. – Invariant mass distribution of selected $B_c^+ \to J/\psi\pi^+$ (bottom) and $B_c^+ \to J/\psi\pi^+\pi^-\pi^+$ (top) candidates used in the branching fraction determination of the $B_c^+ \to J/\psi\pi^+\pi^-\pi^+$ decay mode. The fits to the data are superimposed.

However, the larger number of tracks in the final state results in a reduced efficiency due to the detector geometrical acceptance, and to the tracking and selection efficiencies.

Theoretical predictions can be tested by measuring the branching fraction of $B_c^+ \to J/\psi\pi^+\pi^-\pi^+$ relative to that of $B_c^+ \to J/\psi\pi^+$.

As for the previous analysis, the online selection relies on trigger lines dedicated to (di)muon selection, providing good efficiency for events with $B_c^+ \to J/\psi\pi^+$ or $B_c^+ \to J/\psi\pi^+\pi^+\pi^+$, where $J/\psi \to \mu^+\mu^-$. The offline selection is very similar to that used in the production cross section measurement, including the B_c^+ requirements on the transverse momentum ($p_T > 4.0\,\mathrm{GeV}/c$) and on the decay time ($\tau > 0.25\,\mathrm{ps}$).

Other sensitive variables are: the smallest χ^2_{IP} among the pion candidates, the B_c^+ vertex χ^2_{vtx} per degree of freedom, the B_c^+ candidate impact parameter significance, and the cosine of the largest opening angle between J/ψ and pion candidates in the plane transverse to the beam. The latter peaks at positive values for signal as the B_c^+ meson has a high transverse momentum. Background events originating from combination of tracks from different B mesons peak at negative values, whilest combinatorial background events that include random combinations of tracks are uniformly distributed. These four discriminating variables are combined in a likelihood test. The signal hypothesis is described using a Monte Carlo simulation of $B_c^+ \to J/\psi\pi^+$ and $B_c^+ \to J/\psi\pi^+\pi^-\pi^+$ decays, while for background far-sidebands are used considering B_c^+ candidates with mass in the range 5.35–5.80 GeV/c^2 or 6.80–8.50 GeV/c^2.

Requirements on the log-likelihood ratio have been chosen to maximize the signal significance in the signal mass region ($\pm 2.5\sigma$ around the B_c^+ nominal mass).

The selected samples are shown in fig. 2. The superimposed models describe the signals with a Gaussian, having position and width fitted to data, while the background is assumed to be an exponential function with a second order polynomial as argument.

We observe 135 ± 14 $B_c^+ \to J/\psi\pi^+\pi^-\pi^+$ and 414 ± 25 $B_c^+ \to J/\psi\pi^+$ signal events. As for the previous analysis, the relative selection efficiency for the two channels is determined using a simulation. An additional source of uncertainty on the determined efficiency ratio comes from the model chosen to simulate the signal sample. Among the

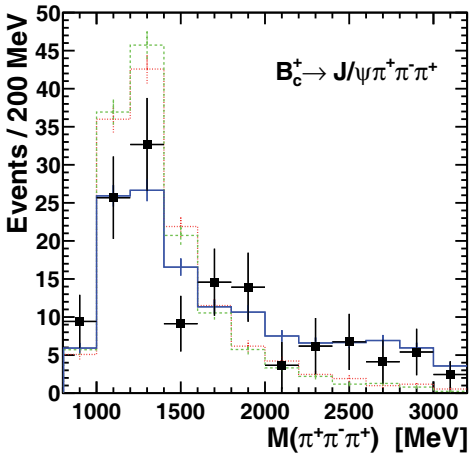

Fig. 3. – Invariant mass distribution of the $\pi^+\pi^-\pi^+$ combinations for sideband-subtracted $B_c^+ \to J/\psi\pi^+\pi^-\pi^+$ data (points) and signal simulation (lines). The solid blue line corresponds to the BLL simulations, the PH and PHPOL models are shown as a green and red dashed line, respectively.

models used to simulate $B_c^+ \to J/\psi\pi^+\pi^-\pi^+$, the phenomenological model by Berezhnoy, Likhoded and Lushinsky [18] is based on amplitude factorization into hadronic and weak currents, implements $B_c^+ \to J/\psi W^{+*}$ axial-vector form-factors and a $W^{+*} \to \pi^+\pi^+\pi^+$ decay via the exchange of virtual $a_1^+(1260)$ and $\rho^0(770)$ resonances. Since it is not possible to identify which of the same-sign pions originates from the ρ^+ decay, the two ρ^0 paths interfere. Two other phase-space models, implementing the same decay chain with no interference and with either no polarization in the decay (PH) or helicity amplitudes of 0.46, 0.87, and 0.20 for +1, 0 and −1 J/ψ helicities (PHPOL).

Comparing the invariant mass of the three pions (shown in fig. 3 as an example), the invariant mass of $\pi^+\pi^-$ pairs (with two entries per event), and the J/ψ polarization angle, it was concluded that the BLL model gives the best overall description of data, and is therefore used to evaluate the central value of the efficiency ratio. Phase-space models are used to asses model-dependence systematic uncertainties.

The branching fraction ratio results

$$\frac{\mathcal{B}(B_c^+ \to J/\psi\pi^+\pi^-\pi^+)}{\mathcal{B}(B_c^+ \to J/\psi\pi^+)} = 2.41 \pm 0.30 \pm 0.33,$$

where the first uncertainty is statistical and the second systematic.

Different theoretical calculations predict this ratio between 1.5 and 2.3 [19, 18]. It is also consistent with the $\mathcal{B}(B^+ \to \bar{D}^{*0}\pi^+\pi^-\pi^+)/B(B^+ \to \bar{D}^{*0}\pi^+) = 2.00 \pm 0.25$ [5] which is mediated by similar decay mechanisms and a similar ratio of phase-space factors.

This result constitutes the first test of theoretical predictions for branching fractions of B_c^+ decays.

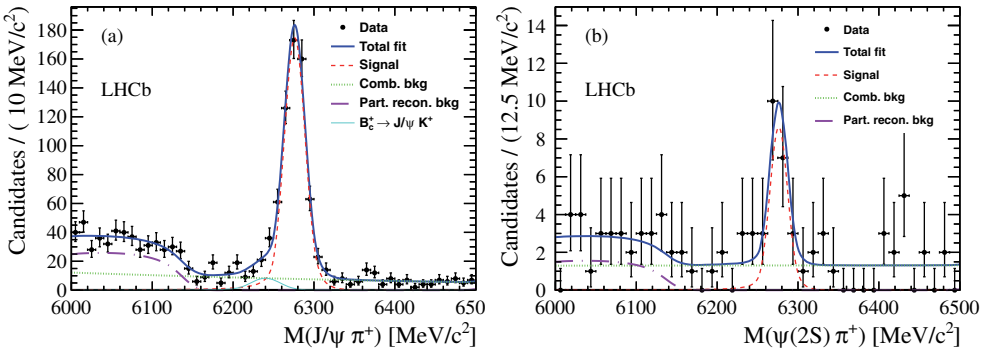

Fig. 4. – Invariant mass distribution of selected (a) $B_c^+ \to J/\psi\pi^+$ candidates and (b) $B_c^+ \to \psi(2S)\pi^+$ candidates. The fits to the data are superimposed.

5. – Observation of the decay $B_c^+ \to \psi(2S)\pi^+$

The decay $B_c^+ \to \psi(2S)\pi^+$, with $\psi(2S) \to \mu^+\mu^-$ is observed for the first time with $1.0\,\text{fb}^{-1}$ of pp collision data collected in 2011 at $\sqrt{s} = 7\,\text{TeV}$, with significance of 5.2σ. The branching fraction of $B_c^+ \to \psi(2S)\pi^+$ relative to that of $B_c^+ \to J/\psi\pi^+$ is measured to be $0.250 \pm 0.68 \pm 0.014 \pm 0.006$ where the first uncertainty is statistical and the second systematic. The third term is the uncertainty on the ratio $\mathcal{B}(\psi(2S) \to \mu^+\mu^-)/\mathcal{B}(J/\psi \to \mu^+\mu^-)$.

Following a loose preselection, requiring high muon p_T, detachment of the pion track from the primary vertex, good vertex fit and a mass for the B_c^+ candidate within a $0.5\,\text{GeV}/c^2$ mass window around the world average [5], a boosted decision tree (BDT) is used to perform further background suppression.

The variables used as input for the BDT are chosen to be well discriminating between signal and background, and to have similar distributions for $B_c^+ \to \psi(2S)\pi^+$ and $B_c^+ \to J/\psi\pi^+$ channels. The similarity of distributions causes the systematics to cancel when evaluating the branching fraction. Vertex quality, pointing and detachment variables, B_c^+ transverse momentum are used as discriminating variables.

The samples used for the BDT training are obtained from Monte Carlo simulations for the signal, and from far B_c^+ mass sidebands for the background. The background sample is taken from pre-selected data with the B_c^+ candidate reconstructed mass in the range $6164 < M_{B_c^+} < 6206\,\text{MeV}/c^2$, or $6346 < M_{B_c^+} < 6388\,\text{MeV}/c^2$.

The BDT is then applied to data. A selection cut on the BDT response is applied. The threshold is optimized in order to maximize the $B_c^+ \to \psi(2S)\pi^+$ signal significance as estimated using Monte Carlo and sidebands.

The invariant mass distributions of B_c^+ candidates reconstructed as $B_c^+ \to J/\psi\pi^+$ and $B_c^+ \to \psi(2S)\pi^+$ are shown in fig. 4.

The number of signal events are obtained by fitting the B_c^+ mass spectrum in fig. 4. As for the previous analysis, the signal is modeled with a double-sided Crystal Ball function. The combinatorial background is modeled with an exponential function, while partially reconstructed backgrounds, in the low-mass region, are modeled with a resolved Argus function [20]. Contribution from the Cabibbo-suppressed $B_c^+ \to J/\psi K^+$ decay mode to the $B_c^+ \to J/\psi\pi^+$ mass spectrum is modeled with a Crystal Ball function whose parameters are fixed to values obtained from the simulation.

The observed numbers of signal candidates are 595 ± 29 for the $B_c^+ \to J/\psi\pi^+$ channel and 20 ± 5 for $B_c^+ \to \psi(2S)\pi^+$; corresponding to a significance if 5.2σ.

The ratio of yields is $N_{B_c^+ \to \psi(2S)\pi^+}/N_{B_c^+ \to J/\psi\pi^+} = 0.034 \pm 0.009\,(\text{stat})$.

The total efficiency, including the detector acceptance, the trigger, reconstruction and selection efficiencies has been determined using simulated events for the two channels and found to be $\varepsilon_{B_c^+ \to \psi(2S)\pi^+}/\varepsilon_{B_c^+ \to J/\psi\pi^+} = 1.040 \pm 0.009$ where the uncertainty is due to the limited size of the Monte Carlo sample.

The dominant systematic effect is due to the choice of threshold on the BDT response, a 4.5% uncertainty has been assessed.

Other considered systematic effects are related to the choice of the signal and background model, accounted for as 1.7% and 2.9% uncertainties, and to possible data-simulated distributions disagreement, found to be negligible compared to statistical fluctuations. The total systematic uncertainty is 5.7%.

To conclude, the ratio of branching fractions is measured to be

$$\frac{\mathcal{B}(B_c^+ \to \psi(2S)\pi^+,\ \psi(2S) \to \mu^+\mu^-)}{\mathcal{B}(B_c^+ \to J/\psi\pi^+,\ J/\psi \to \mu^+\mu^-)} = 0.033 \pm 0.009(\text{stat}) \pm 0.002(\text{syst}).$$

Taking $\mathcal{B}(J/\psi \to e^+e^-) = (5.94 \pm 0.06)\%$ and $\mathcal{B}(\psi(2S) \to e^+e^-) = (7.73 \pm 0.17) \times 10^{-3}$ and assuming universality of the electroweak interaction, we obtain

$$\frac{\mathcal{B}(B_c^+ \to \psi(2S)\pi^+)}{\mathcal{B}(B_c^+ \to J/\psi\pi^+)} = 0.250 \pm 0.068(\text{stat}) \pm 0.014(\text{syst}) \pm 0.006(\mathcal{B}),$$

where the last term represents the uncertainty on $\mathcal{B}(\psi(2S) \to \mu^+\mu^-)/\mathcal{B}(J/\psi \to \mu^+\mu^-)$. This result favours the prediction made by the relativistic quark model [21] with respect to other models.

6. – Conclusion and outlook

The B_c physics is interesting for the study of production mechanism, spectroscopy and decay modes, providing a system, unique in the Standard Model, composed by two different heavy quarks. LHCb has contributed with the world most precise measurements of both the mass and the production cross section of the B_c^+ meson, and observed for the first time the $B_c^+ \to J/\psi\pi^+\pi^-\pi^+$ and $B_c^+ \to \psi(2S)\pi^+$ decays. Offering the first tests of theoretical predictions for branching fractions of the B_c^+ decays.

An important contribution to systematics come often from the uncertainty on the lifetime of the B_c^+ which is one of the LHCb measurement expected for the long technical stop of LHC.

While for the analyses here reported, only 2011 data have been used, the LHCb experiment has now collected $3\,\text{fb}^{-1}$, making possible to access excited states and rarer decays, and to achieve precise branching fraction measurements. Ongoing analyses will keep testing the $\bar{b} \to \bar{c}$ transition decays, but also $c \to s$ transition decays will be probed. Besides, information about the importance of annihilation topologies will be extracted from decays with concurrent Feynman diagrams. In the next years, LHCb will run at increased luminosity exploring the rich physics of B_c states spectroscopy and suppressed B_c decays.

REFERENCES

[1] Brambilla N. *et al.* (QWG), arXiv:hep-ph/0412158 and reference therein
[2] Chang and Wu, *Eur. Phys. J. C*, **38** (2004) 267.
[3] Godfrey S., *Phys. Rev. D.*, **70** (2004) 05401.
[4] Brambilla N. and Vairo A., *Phys. Rev. D.*, **62** (2000) 094019.
[5] Beringer J. *et al.* (Particle Data Group), *Phys. Rev. D*, **86** (2012) 010001.
[6] Zhenwei Yang, talk presented at this conference.
[7] Alves Jr. A. A. *et al.* (The LHCb Collaboration), *J. INST*, **3** (2008) S08005.
[8] Aaij R. *et al.* (The LHCb Collaboration), *Phys. Rev. Lett.*, **109** (2012) 232001.
[9] Skwarnicki T., *DESY*, **1986** (F31-86-02).
[10] Aaij R. *et al.* (The LHCb Collaboration), *Phys. Rev. D*, **85** (2012) 091105.
[11] Chang C. H., Wang J. X. and Wu X. G., *Comput. Phys. Commun.*, **174** (2006) 241.
[12] Sjöstrand T., Mrenna S. and Skands P. Z., *J. High. Energy Phys.*, **05** (2006) 026.
[13] Lange D. J., *Nucl. Instrum. Methods Phys. Res. A*, **462** (2001) 152.
[14] Golonka P. and Was Z., *Eur. Phys. J. C*, **45** (2006) 97.
[15] Abe F. *et al.* (The CDF Collaboration), *Phys. Rev. Lett.*, **97** (2006) 012002.
[16] Abazov V. *et al.* (The D0 Collaboration), *Phys. Rev. Lett*, **102** (2009) 092001.
[17] Aaij R. *et al.* (The LHCb Collaboration), LHCB-PAPER-2012-054, arXiv:1303.1737.
[18] Likhoded A. K. and Lushinsky A. V., *Phys. Rev. D*, **81** (2010) 014015.
[19] Rakitin A. and Koshkarev S., *Phys. Rev. D*, **81** (2010) 014015.
[20] Albrecht H. *et al.* (The Argus Collaboration), *Phys. Lett. B*, **241** (1990) 278.
[21] Ebert D., Faustov R. and Galkin V., *Phys. Rev. D*, **68** (2003) 094020.